Exploring scale-effects on water balance components and water use efficiency of toposequence rice fields in Northern Italy

A. Facchi, M. Rienzner, S. Cesari de Maria, A. Mayer, E. A. Chiaradia, D. Masseroni, S. Silvestri and M. Romani

ABSTRACT

Water use efficiencies (WUEs) between 20% and 60% are commonly reported for single rice paddies. When larger spatial domains are considered, higher WUE than minimum values observed for individual fields are expected due to water reuse. This study investigates scale-effects on water balances and WUEs of four adjacent rice fields located in Northern Italy and characterized by different elevations ($A \cong B + C > D$). Water balance terms for the paddies were quantified during the agricultural season 2015 through the integrated use of observational data and modelling procedures. Following a Darcy-based approach, percolation was distinguished from net seepage. Results showed net irrigation of about 2,700 and 2,050 mm for fields A and B, and around 640 and nearly 0 mm for C and D. WUE of A, B, C and D amounted, respectively, to 21, 28, 66 and >100%. Values for C and D were due to less permeable soils, to seepage fluxes providing extra water inputs and to the shallow groundwater level. When the group of paddies ACD was considered (B was not included since it was separated by a deep channel), net irrigation and WUE were found to reach 1,550 mm and 39%, confirming the important role of water reuses in paddy agro-ecosystems.

Key words | rice, percolation, seepage, toposequence, water balance terms, water use efficiency

A. Facchi (corresponding author)
M. Rienzner
S. Cesari de Maria
A. Mayer
E. A. Chiaradia
D. Masseroni
Department of Agricultural and Environmental Sciences (DiSAA),
Università degli Studi di Milano,
Via Celoria 2, 20133, Milano (MI),
Italy
E-mail: *arianna.facchi@unimi.it*

S. Silvestri
M. Romani
Centro Ricerche sul Riso,
Ente Nazionale Risi (ENR),
Strada per Ceretto 4, 27030, Castello d'Agogna (PV),
Italy

INTRODUCTION

Rice is one of the most important food crops worldwide, and the last FAO statistics show that rice ranked second in food and agricultural commodities, with a global production of more than 700 million tons per year (FAOSTAT 2013). Italy is the largest rice producer in Europe, with the majority of production concentrated in the Po river plain (Northern Italy), in a vast area between Lombardy and Piedmont (about 250,000 hectares).

As is widely known, rice cropping systems generally require copious amounts of water when traditional irrigation management is adopted, due to the continuous flooding of rice paddies from seeding to a couple of weeks before harvest in order to maintain a ponded water level of 5–10 cm over the soil (Bouman *et al.* 2007; Cesari de Maria *et al.* 2017). Owing to this peculiar water management, rice usually requires from two to three times more water than other cereals, such as wheat or maize (Tuong *et al.* 2005). However, water use for flooded rice (i.e., the sum of irrigation and rainfall) may vary significantly due to the site characteristics, ranging from a relatively low value of 650–850 mm for some Asian paddies (e.g., Tabbal *et al.* 2002; Cabangon *et al.* 2004) up to more than 2,500 mm observed in European experiments (e.g., Aguilar & Borjas 2005; Cesari de Maria *et al.* 2017). Nevertheless, almost all the literature regarding water use and water balance of rice fields relates to studies performed in Asia, where

doi: 10.2166/nh.2018.125

puddling (i.e., harrowing or rotavating under shallow submerged conditions) is performed to reduce soil permeability, and only very few references focus on European rice cropping systems (Aguilar & Borjas 2005; Playán *et al.* 2008; Zhao *et al.* 2015; Cesari de Maria *et al.* 2017), which are very different with respect to climate, soil types, rice varieties, irrigation management and agronomic practices. Consequently, there is the need to fill this research gap and to provide numbers to European water resource managers and to the public, who accuse the rice cultivation industry of being excessively water-consuming.

There are numerous factors influencing the water balance terms in a paddy, such as irrigation management, land preparation method, layout of the field, soil characteristics, agronomic management, crop characteristics, groundwater depth, rainfall amount and timing, and the evaporative power of the atmosphere resulting from climatic conditions. Many water balance terms can be directly measured in the field (i.e., rainfall, irrigation inflow, irrigation outflow, water storage within and above the soil, evapotranspiration) as shown, for instance, in Cesari de Maria *et al.* (2017). The residual term of the water balance equation (*SP*) can be considered as the sum of two processes: net percolation, which is the net vertical flux at the bottom of the soil volume (mainly directed downward, since the continuous water flux toward the groundwater table basically prevents capillary rise into the root zone in flooded rice fields); and net seepage, defined as the subsurface flow of water (losses plus incoming fluxes) throughout the bunds (Bouman *et al.* 2007). In flooded rice fields, seepage is influenced by many factors, such as the position and slope of soil layers, their hydraulic conductivity, the presence of drains and their characteristics, the characteristics of bunds surrounding the field (thickness, presence of cracks, lining) and the water table depth and velocity (FAO 1979). On the other hand, percolation is mostly influenced by the resistance to water movement in the soil profile, which is mainly governed by the saturated conductivity of the plough pan (Bouman *et al.* 2007) and by the difference in water head along the vertical profile.

Compared to the other terms of the water balance, *SP* is the one most affecting rice water requirements. In general, the literature reports that total *SP* in a paddy may vary between 25% and 50% of the water inputs (i.e., irrigation plus rainfall) with heavy soil and groundwater depth within 0.5 m (Cabangon *et al.* 2004; Dong *et al.* 2004), and 80% in coarse-textured soil with a groundwater table deeper than 1.5 m (Sharma *et al.* 2002; Singh *et al.* 2002).

Since *SP* cannot be measured directly in field-scale experiments and is usually obtained as the residual term of the water balance, it is a challenge for research to separate *SP* into the two fluxes. According to Wopereis *et al.* (1994), the soil vertical profile some days after flooding can be described as a sequence of layers. Following a downward order, the layers are: (i) ponding water, (ii) muddy layer with low resistance to water flow, (iii) plough sole layer with a relevant resistance to water flow, and (iv) subsoil layer scarcely affected by agronomical practices. After flooding, the muddy layer and the plough sole are saturated; in this condition, the percolation rate P can be predicted by the Darcy's equation (Rizzo *et al.* 2013). This approach is commonly adopted in the literature and it is implemented, among others, in the Darcy-based soil-water balance model SAWAH (Simulation Algorithm for Water Flow in Aquatic Habitats; Ten Berge *et al.* 1992) to calculate the amount of water that percolates from paddy fields.

A widely adopted indicator to measure the efficiency of an irrigated system is the water use efficiency (WUE), which is obtained as the ratio of evapotranspiration to water inputs (i.e., irrigation plus rainfall). Tuong & Bhuiyan (1999) reported that WUE of flooded rice can be as low as 20%, although with remarkable variations (upper bound of the range is 60%). Since *SP* generally increases the field irrigation requirements of a rice paddy, WUE of a single field is strongly influenced by the water amount lost by *SP*. When focusing on larger spatial domains, WUE is expected to increase compared to the minimum values found for single paddies, due to the possible water reuse within the system. Hafeez *et al.* (2007) and Wallace (2000) reported increased values of water use indicators considering, respectively, the district and the catchment scales. At a larger scale than the single field, *SP* outflowing from fields can be partially collected by ditches, thus increasing the irrigation discharge available for downhill paddies. Additionally, *SP* can also represent a direct water input to fields at a lower elevation, due to seepage through the bunds. In rain-fed rice, Tsubo *et al.* (2006) observed that water losses by lateral movements were greater in the upper part of the rice field

toposequence, and that these lateral fluxes represented a possible water gain for fields at a lower elevation, also affecting their field WUE. Similarly, Schmitter *et al.* (2015) found that the field position in the toposequence influenced the crop water productivity in the case of irrigated rice, due to subsurface lateral fluxes that represented extra water input for the lower lying fields. Moreover, lower paddies may benefit from a higher groundwater level that plays an important role in reducing percolation fluxes when groundwater is shallow (FAO 1979; Cesari de Maria *et al.* 2016, 2017).

Hence, in paddy areas, topography is a factor activating water exchanges and reuse between paddies. For this reason, WUE of a single rice field in a toposequence tends to be poorly representative of the overall efficiency of the paddy system, especially in areas characterized by shallow groundwater, due to the strong interactions that may occur among fields. In spite of its relevance, this issue is still not much investigated in the literature and, to the authors' knowledge, no experiments leading to a quantification of water fluxes and WUE for paddies in a toposequence have been conducted in European rice areas.

The aim of this paper is to provide procedures and elements for the investigation of scale-effects when considering the water balance terms and the WUE of flooded rice systems in a toposequence. To reach the objective, the water balance terms of four rice paddies characterized by different elevations and located in the most important paddy area in Italy (Lomellina rice district, Northern Italy) were quantified through the integrated use of observational data and modelling procedures. Net irrigation discharges, percolation and seepage fluxes of the four fields are discussed with respect to their position in the toposequence, together with WUEs considering both the single-field scale and the group of rice paddies.

MATERIAL AND METHODS

Description of the site

The study was carried out at the Cerino rice farm (Semiana, Pavia) located in Lomellina, a historic rice district situated in the Western Lombardy plain, southwest of the city of Milan. The area is characterized by a humid subtropical climate (Cfa) according to the Köppen climate classification. Considering the period 1993–2015, the mean temperature in the months from April to September is around 19.6 °C, while the total rainfall is about 310 mm. The average daily reference evapotranspiration (ET_0) of the same period, as calculated from Allen *et al.* (1998), is 3.6, 4.5, 5.2, 5.8, 4.2, 3.1 mm d^{-1}, respectively.

The monitoring activity was performed in 2015 in three adjacent paddy fields, named A, C and D, and in an additional field, named B, separated from the others by a deep drainage channel. The area of the four fields (A, B, C, D) is, respectively, 7.8, 8.2, 4.8 and 5.8 ha. The elevation of the fields decreases from A (94.0 m a.s.l.), to C (about 1 m below A), and D (about 0.5 m below C); B has an elevation of 93.8 m a.s.l. Figure 1 shows a plan view and cross sections of the study area. In the rice district of Northern Italy, bunds are permanent (not ploughed) and decades of clogging due to the flooding practice generally make them rather impervious. In the experimental farm, bunds surrounding the block of fields ACD (apart from the southern one), and field B (apart from the northern one) are about 5 m in size at the seedbed level, and often flanked by farm roads, as can be seen in Figure 1. The remaining bunds are thinner, with a thickness of about 2 m at the seedbed level.

Before sowing, the four paddies were harrowed and subsequently rolled. Fields A and B were planted with the rice variety Sole CL, while fields C and D were planted with the variety CL 15. Both the varieties are characterized by a growing cycle of 135–140 days.

A different irrigation management method was adopted for the four paddies: water seeding and continuous flooding (WFL) was applied in C and D, while dry seeding and delayed flooding (i.e., direct seeding on dry soil followed by a delayed flooding when the crop reaches the 3–4 leaf stage; DFL) was adopted for A and B. After submersion, the ponding water was maintained in all the fields for approximately the entire growing cycle, except for short periods when agronomic operations were conducted. In particular, a first dry period was necessary in fields C and D to allow root development and, successively, dry periods were performed for all the fields to allow the application of fertilizers and pesticide treatments. Figure 2 illustrates

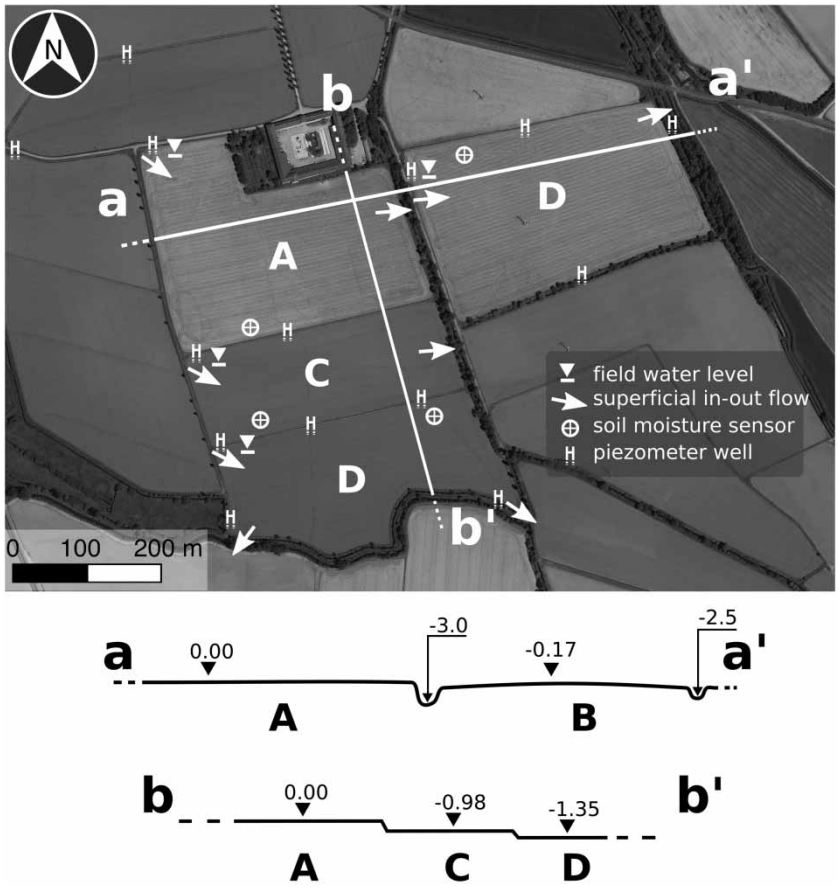

Figure 1 | Plan view and cross sections of the monitored fields with the position of the installed instruments.

flooding periods (dots) and seeding and harvesting dates (x) of the four paddies. Despite the different irrigation management of fields A and B compared to C and D, the overall length of the flooding period was approximately the same for the four fields.

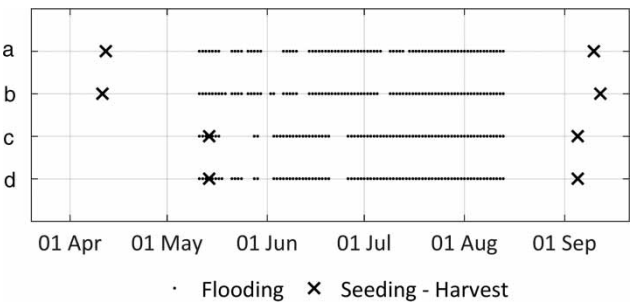

Figure 2 | Flooding periods and seeding and harvesting dates for paddies a, b, c and d in the agricultural season 2015 at the Cerino rice farm (Semiana, Pavia).

Experimental setup and data collection

For investigating the water dynamics within the four fields, a sensor network was set up in each field (Figure 1) to monitor the following water fluxes and storages: irrigation inflow, irrigation outflow, ponding water height, soil water content and water table depth. All the measurements were continuously recorded by different data loggers during the whole crop cycle, with a time step of 10 to 30 minutes.

Irrigation inflows and outflows at each field were measured by long-throated flumes equipped with a level gauge (Chiaradia *et al.* 2015). The flumes were self-made, and dimensioned to fit the expected maximum discharge of 80 L s^{-1} (rectangular-shaped, 1.2 m long, 0.3 m wide and 0.4 m high). Flow rate curve was estimated by using the WinFlume software (U.S.B.R., USA). Upstream water levels were measured in stilling wells by pressure

transducers having a full scale of 0.30 bar (Keller, Switzerland). A total of nine long-throated flumes were installed: four to measure irrigation inflows at the four fields, and five for monitoring the irrigation outflows (field D has two irrigation outlets).

The ponding water height was measured by pressure transducers (full scale of 0.30 bar; Keller, Switzerland) installed in the four fields. The soil water content was monitored in each field at four soil depths (10, 30, 50, 70 cm) by multi-level FDR (frequency domain reflectometry) probes (EnviroSCAN, Sentek, Australia).

Water table depth was monitored through a total of 14 piezometers made by windowed 1″1/5 PVC pipes installed into holes drilled using a manual auger. Twelve piezometers were equipped with a pressure transducer (Keller, Switzerland; STS, USA; Van Essen Instrument, The Netherlands), while the two remaining were monitored weekly through manual measurements. For each monitoring time step, the measured groundwater levels were interpolated on a regular grid with 10 m × 10 m cells (Natural Neighbor Interpolation method; MATLAB, Mathworks, USA).

Between March and May 2015, a geophysical survey with an EMI device (GSSI Profiler-EMP400) and a traditional soil survey (40 drillings carried out with a manual auger) were conducted to obtain a preliminary description of soil physical characteristics and distribution. For each drilling, disturbed soil samples were taken at three depths (0–30, 40–80 and 90–130 cm) for textural analysis. Soil of the four fields shows a significant uniformity in the tilled horizon (top 30 cm), with a sandy loam texture, whereas a higher textural variability (from sandy to silty clay loam) is evident below this horizon. All the information collected in the preliminary soil survey was used to identify areas potentially characterized by different soil types and to select the more representative sites for an in-depth soil characterization. In November 2015, five 2 m-deep soil profiles were opened with an excavator and characterized (two profiles in field A, two in field B and one in field C). Disturbed soil samples were taken from each soil horizon for chemical-physical soil routine analysis, and undisturbed soil samples were collected at the same positions for the determination of bulk density. Large undisturbed soil cores (height 15.0 cm, ø 14.6 cm, two replicates) were taken from the less conductive layer (LCL) of each profile (often being the hardpan) for the laboratory determination of the saturated soil hydraulic conductivity. Depth and thickness of LCL were observed for each profile by considering different features (e.g., soil compaction, transition between layers showing reductive features above – and oxidative conditions below).

The soil survey highlighted a narrow area crossing the central part of field B, characterized by a relatively coarser soil with respect to the other two portions of the field. Unfortunately, a soil profile was not opened in this area, but information about LCL position and texture could be obtained by drillings.

In field D, drainage is strongly impeded and water is ponding on the soil surface for nearly the whole year; therefore, it was impossible to open a profile in November 2015. However, the preliminary soil survey and the installation of piezometric wells allowed the detection of a thick and compact clayey layer about 1.2 m below the soil surface, which acts as the LCL and is most likely responsible for the poor drainage of field D.

Finally, hourly meteorological data (air temperature and humidity, rainfall, wind speed, solar radiation) were obtained by the closest regional weather station, 12 km from the experimental site.

Calculation of balance terms

For each field, a balance equation (Equation (1)) was implemented at an hourly time step from dry seeding until harvest in the case of DFL treatments (A and B), and from the first flooding before wet seeding until harvest for WFL ones (C and D). A field control volume ranging from the top of the ponding water to the bottom of the LCL was considered (this means that control volumes are different for the four fields, see Table 1).

$$\Delta S_{w,t} + \Delta S_{s,t} = Q_{in,t} - Q_{out,t} + R_t - ET_t + SP_t \quad (1)$$

where t is the time index (h); ΔS_w is the variation in the ponding water height; ΔS_s is the variation of the soil water storage; Q_{in} and Q_{out} are the irrigation inflow and outflow divided by the field area; R is the rainfall; ET is the evapotranspiration from soil/ponding water (evaporation) and crop (transpiration); SP is the seepage and percolation

Table 1 | Main soil physical and hydrological properties of LCLs of the fields

Field	Field fraction	d (cm)	L (cm)	Ks (cm d^{-1})	Texture	BD (g cm^{-3})
A	0.23	30	5	0.342	Sandy loam	2.05
	0.77	55	25	1.020	Loam	2.00
B	0.30	20	5	0.017	Sandy loam	1.98
	0.37	20	15	1.700[a]	Sandy loam	–
	0.43	40	15	0.145	Loam	1.93
C	1.00	45	7	0.057	Loam	1.98
D	1.00	120	40	0.001[a]	Clay loam	–

[a]estimated.
d, depth; L, thickness; Ks, saturated hydraulic conductivity; BD, bulk density.
Texture following USDA classification.

term discussed in the Introduction. All the terms are in mm h^{-1}. Positive signs indicate an increasing storage or a flux entering the soil volume in the time step. Seepage and percolation (SP) can be split as follows:

$$SP_t = Se_t - P_{bal,t} \tag{2}$$

where Se (mm h^{-1}) is the seepage flux, positive when the inflow is higher than the outflow, and P_{bal} (mm h^{-1}) is the vertical flux at the bottom of the LCL, that can be both negative (downward) and positive (upward). However, in flooded fields, a continuous downward flow of water from the soil surface to below the LCL (called 'percolation') basically prevents capillary rise, and a positive vertical flux is found only in the case of high-pressure groundwater below the LCL. On the contrary, when paddies are dry, the flow at the bottom of the LCL can become positive (capillary rise) if the water table is sufficiently shallow.

Most of the terms in Equation (1) were measured, while the remaining terms were calculated as described hereafter. ET was estimated following the FAO single crop coefficient approach (Equation (3)) (Allen *et al.* 1998), considering a complete fulfilment of the crop evapotranspiration requirements:

$$ET_t = K_{c,t} \cdot ET_{0,t} \tag{3}$$

The reference evapotranspiration (ET_0) was computed from hourly meteorological data following Allen *et al.* (2006), while time-varying crop coefficients (K_c) were obtained for the two irrigation managements, WFL ($Kc_{ini} = 0.8$, $Kc_{mid} = 1.1$, $Kc_{end} = 0.6$) and DFL ($Kc_{ini} = 0.6$, $Kc_{mid} = 1.1$, $Kc_{end} = 0.6$) from a former experiment carried out on rice under the same irrigation treatments in a study site nearby (12 km) (Chiaradia *et al.* 2015; Cesari de Maria *et al.* 2017).

The SP term was not monitored and it was obtained by applying Equation (1). Furthermore, if one of the two components, Se or P_{bal}, can be estimated independently, then Equation (2) can be applied to estimate the other one.

An estimation of the percolation P_{bal} was obtained, in this study, by applying the 1D Darcy's equation (Equation (4)) during the field submersion (ponding water on the soil surface >0), when most of the percolation is expected to occur:

$$P_{D,t} = b \cdot K_s \cdot \frac{\Delta H_t}{L} \tag{4}$$

where P_D is the percolation (mm h^{-1}) calculated from the Darcy's law; Ks is the saturated hydraulic conductivity of LCL (cm d^{-1}); L is the thickness of LCL (cm); b is a conversion factor (10/24 mm d cm^{-1} h^{-1}); and ΔH (cm) is the difference in the total hydraulic head at the two LCL sides:

$$\Delta H_t = H_{2,t} - H_{1,t} \tag{5}$$

where H_1 (cm) and H_2 (cm) are the total hydraulic heads at the top and the bottom of the LCL, respectively.

For fields characterized by different soil zones (i.e., A and B), the total percolation was obtained by weighing the percolation fluxes obtained for the different soil zones by their surface areas.

The LCL properties (Ks and L) were investigated for the soil profiles representative of the different soil zones; in particular, Ks was determined on large undisturbed soil cores by applying the core method in the laboratory (e.g., Reynolds & Elrick 2002). The hydraulic heads H_1 and H_2 were estimated for each soil zone during the flooding period as described hereafter.

Since the muddy layer above the LCL is typically incoherent and highly conductive (Wopereis *et al.* 1994), its effect on the flux can be neglected in computing Equation

(4). When the LCL is deeper than 30 cm, a soil layer may be placed between the incoherent muddy layer and the LCL, but also its effect on the percolation can be neglected since its *Ks* is usually higher than the LCL by far.

With respect to Figure 3, when the reference level $z = 0$ is placed at the bottom of the LCL, the total hydraulic head at the top of the LCL (H_1) can be approximated as:

$$H_{1,t} = w_t + d + L \tag{6}$$

where w (cm) is the height of the ponding water; d (cm) is the depth of the LCL from the soil surface; and L (cm) is its thickness. All the quantities on the right-hand side of Equation (6) were measured in the field.

The total hydraulic head at the bottom of the LCL (H_2) was computed according to the water table position with respect to LCL, as shown in Figure 3.

In the case of unsaturated soil below the LCL (Figure 3, left-hand side), a negative water pressure occurs below the LCL, whereas the LCL is supposed to be fully saturated (i.e., water pressure ≥ 0). Therefore, H_2 being the water pressure at the interface between these layers, its value can be assumed equal to zero.

In the case of a complete saturation of the soil profile (Figure 3, right-hand side), the soil below the LCL is saturated, its pressure head is positive and increases with depth following a hydrostatic pressure gradient and H_2 is equal to the distance between the groundwater level and the bottom of the LCL (Equation (7)):

$$H_{2,t} = d + L - p \tag{7}$$

where $p = (z_s - z_{w,t})$ (cm) is the distance between the soil surface and the groundwater table computed for each time step. In this case, P_D can become positive if $H_2 > H_1$.

Obviously, ΔH values change for the four fields at each monitoring step, as the ponding water height and the groundwater depth fluctuates.

Since a measure of *Ks* was unavailable for the LCL of the soil unit in the central part of field B, an estimation was carried out by calibrating this parameter in order to obtain, at the end of the agricultural season, a P_D value equal to the *SP* cumulative flux, assuming that no net seepage occurred for field B as a consequence of its topographic position (in analogy to what was observed for field A).

Finally, *Ks* and thickness of the LCL in field D were set to reproduce the negligible observed percolation flux; *Ks*, in particular, was set to a very low value.

Table 1 reports the main soil physical and hydrological properties of the LCLs used in the computation of percolation (P_D) through the Darcy's approach. For each row of parameters, Table 1 also reports the fraction of the area of the field they apply to (according to the soil survey described in the previous section).

The approach for computing P_D was applied only in periods when paddy fields were submerged (ponding water on the soil surface >0). In this case, *Se* was estimated from the cumulative $SP - P_D$ curve by manually calibrating a stepwise linear interpolant, the slope of which is equal to the *Se* value in each time step. *Se* values estimated for each step were also evaluated in the light of the observational

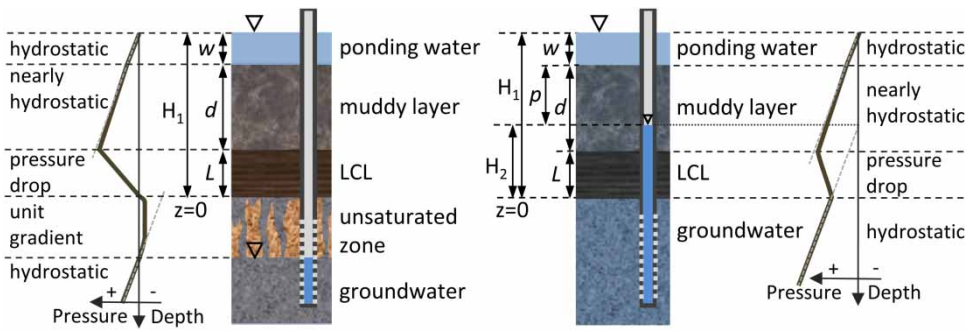

Figure 3 | Scheme of the application of the 1D Darcy's equation in the case the layer below LCL is, respectively, unsaturated (left-hand side) or saturated (right-hand side); qualitative pressure head profiles are also illustrated.

data collected in the field. P_{bal} was consequently set as $SP - Se$. During non-flooding periods (ponding water on the soil surface = 0), the net seepage was assumed to be negligible ($Se = 0$), and the net flux at the bottom of the LCL was obtained as the residual term in the water balance equation ($P_{bal} = SP$; Equation (1)); in this case, positive P_{bal} indicates a capillary rise flux into the soil unit volume. In non-flooding periods, $P_D = P_{bal}$ was furthermore imposed in order to maintain a complete P_D series.

When the group of paddies ACD is considered, the terms of the water balance are calculated from those of the three fields, weighted by their surfaces.

All the equations reported in this section were implemented in a MATLAB script.

Computation of water use efficiencies

The water use efficiency (WUE, %) was calculated for each paddy, as well as for the group of paddies ACD, with the modified index proposed by Dunn & Gaydon (2011):

$$WUE = 100 * \frac{\mathrm{ET}}{\mathrm{Q_{in}} - \mathrm{Q_{out}} + \mathrm{R}} \tag{8}$$

where ET, Q_{in} and Q_{out} are expressed in mm over the whole agricultural season. The irrigation outflow (Q_{out}) was subtracted from the total water inputs (Q_{in}+R) because the irrigation outflow is discharged into the irrigation network and is consequently reused for the irrigation of paddy fields located downslope. It should be noted that the WUE of a group of fields does not correspond to the average of the WUEs of single fields. In particular, the WUE of a group of paddies is reported on the left-hand side of Equation (9), while the area-weighted average of the single WUEs is illustrated on the right-hand side of Equation (9):

$$\frac{\sum A_i \cdot ET_i}{\sum \left[A_i (R + Q_{in,\,i} - Q_{out,\,i})\right]} * 100 \neq \sum \left(\frac{A_i}{A} \cdot \frac{ET_i}{R + Q_{in,\,i} - Q_{out,\,i}} \right) * 100 \tag{9}$$

where A_i is the area of the single fields (m^2), while A is the area of the group of fields (m^2). All the remaining terms (ET, R, Q_{in}, Q_{out}) are also expressed in metres.

RESULTS AND DISCUSSION

Monthly water balance terms

Water balance terms are presented in Figure 4 at a monthly time scale; water volumes entering the fields have positive values, while outgoing volumes have negative values. Some terms are only slightly visible (e.g., ΔS_s and ΔS_w), but all are reported for the sake of completeness. During the flooding period, average groundwater depths at the experimental site were found to be around 0.8, 1.2, 0.1 and 0.6 m in fields A, B, C and D, respectively.

In Figure 4, fields A and B (DFL) show a very similar pattern characterized by large water fluxes mostly due, inward, to the irrigation supply (Q_{in}) and, outward, to the seepage and percolation term (SP). Evapotranspiration (ET) is smaller than Q_{in} and the irrigation outflow (Q_{out}) is nearly absent. The amounts reached by Q_{in} and SP during the season follow the number of flooding days, reaching a maximum in July (Figure 2). The maximum of ET, also occurring in July, is due to the meteorological factors affecting ET_0. Finally, the storage terms (ΔS_s and ΔS_w) have negative values at the start of the season (i.e., water is stored on and within the soil) and positive at drying (i.e., the stored water is released). Field C (WFL) shows common features to A and B, but with remarkably smaller Q_{in} and SP fluxes. Moreover, Q_{out} is often rather relevant in this field, especially in August. The pattern of fluxes in field D (WFL) is different with respect to the other monitored fields. Indeed, Q_{in} has the same magnitude of ET and it is often smaller than Q_{out}; the reason for this is a relevant and positive SP flux. The maximum of Q_{in} occurs in May, which is the only month where SP is negative in D, while the maximum positive SP is reached in July. Finally, when the group ACD is considered, water fluxes and storages appear to have an average behaviour between those shown for A and C.

Breakdown of the *SP* term into seepage and percolation fluxes

The complex behaviour identified for the balance terms in the previous section can be better explained by dividing SP, calculated as the residual of the water balance

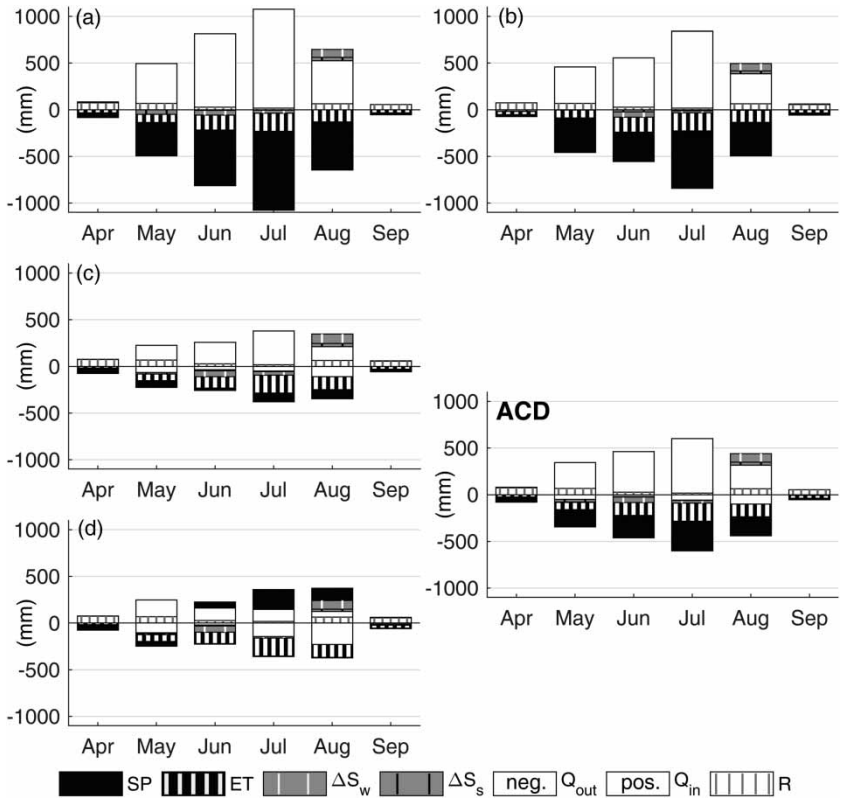

Figure 4 | Monthly cumulated water balance terms for the fields A, B, C, D (panels a, b, c, d, respectively) and the group of fields ACD: SP, seepage and percolation; ET, evapotranspiration; ΔS_w, change in water storage on the field; ΔS_s, change in water storage within the soil; Q_{out}, irrigation outflow (negative); Q_{in}, irrigation inflow (positive); R, rainfall.

(Equation (1), Figure 4), into its vertical and horizontal components, namely, percolation (P_{bal}) and seepage (Se), respectively (Equation (2)).

Figure 5 illustrates SP fluxes cumulated over the agricultural season (bold black line), and P_D fluxes (bold grey line), estimated by applying the Darcy's law. The figure also illustrates the cumulative patterns of Se (dotted black line) and P_{bal} (thin black line) fluxes obtained by partitioning SP. On the X-axis, periods of flooding conditions, as obtained by water level sensors positioned in each field, are additionally reported (the correspondence between these periods and those reported in Figure 1, having the aim of illustrating the water management operated by the farmer, is not always perfect as periods in Figure 1 do not account for short time submersions due to heavy rainfall events on nearly saturated soil).

In the case of field A, a very good correspondence was found between SP and P_D fluxes, with respect to both the cumulative value of the two variables at the end of the season and the seasonal trend. Actually, no incoming seepage was expected in this field due to its high topographic position, and Figure 5(a) suggests that outward seepage can also be considered negligible. Consequently, Se was assumed to be null throughout the season, and thus $P_{bal} = SP$.

For field B (Figure 5(b)), the match between P_D and SP cumulative values at the end of the season is due to the calibration of the Ks value of the coarser soil crossing the central portion of the field. Anyway, the overall seasonal patterns of the two fluxes have a very good match, with SP that does not show sharp short-term deviations from P_D estimation. This allowed the hypothesis of relevant seepage fluxes affecting B to be discarded; these fluxes were set to zero in analogy with field A, also due to a similar position of the two fields with respect to the adjacent fields and to the groundwater level.

The cumulated patterns of SP and P_D for field C (Figure 5(c)) are divergent, due to the presence of relevant seepage fluxes. By comparing the cumulative $(SP - P_D)$

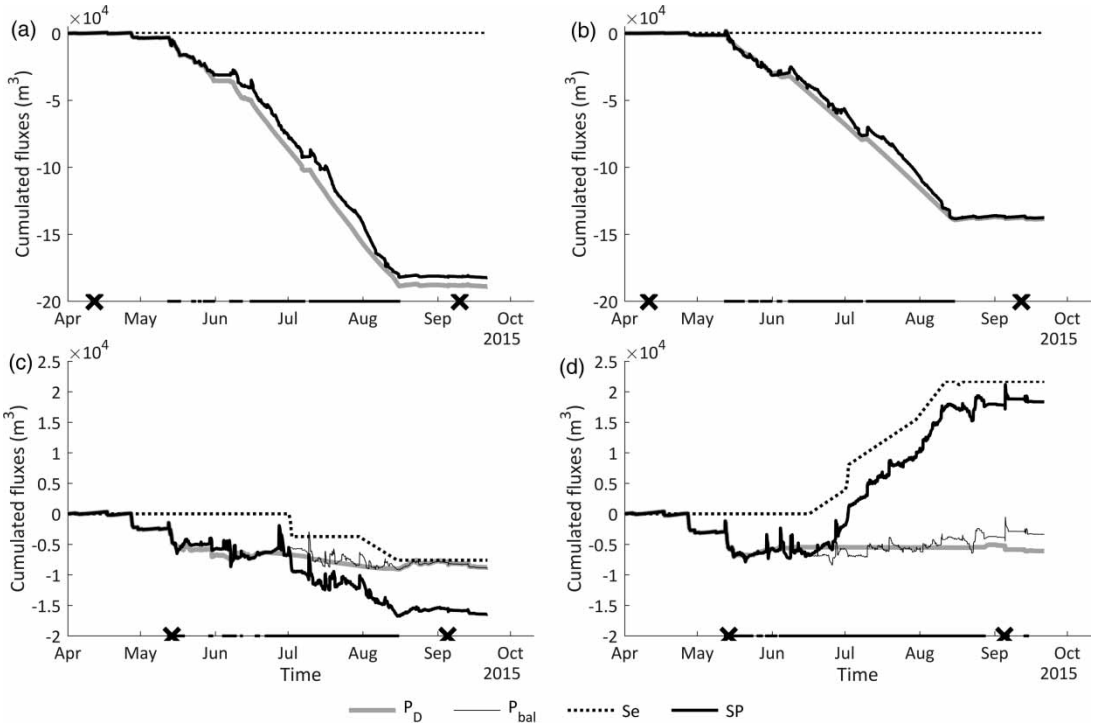

Figure 5 | Daily cumulated fluxes of *SP*, P_D, *Se* and P_{bal} for the fields A, B, C, D (panels a, b, c, d, respectively); panels have different Y scales. On the X axis, black dots show periods with water ponding in the fields, while seeding and harvesting dates are marked with x.

curve for the fields C and D (not shown), a good correspondence between the sudden slope changes in the two lines was evident in different time periods. In particular, changes were found to have the same behaviour but different sign (i.e., a decrease in the curve of field C corresponded to an increase in the cumulative ($SP - P_D$) curve for field D), and this suggested a water flux from C to D in these periods. The first occurrence corresponded to a large break of the embankment between the two fields (about 30 L s^{-1} on average from 1 July 2015 to 2 July 2015) also observed in the field, while the second was a proper seepage flux (about 3 L s^{-1} from 30 July 2015 to 15 August 2015). Both can be noted by observing the *Se* line in Figure 5(c) and 5(d).

Field D was characterized by an irrelevant P_D flux compared to the other three fields (Figure 5(d)); thus, *SP* was mostly due to *Se* during the flooding periods. In addition to the two seepage fluxes coming from C, the cumulated *SP* flux showed an additional rise from 16 June 2015 (1 day after the main submersion in A) to 19 August 2015 (4 days after the drying of fields A and C) with an average flux of 3.0 L s^{-1}. This period was characterized by a groundwater level measured by piezometers on the bund between C and D higher than the ponding water in D (not shown). Therefore, a groundwater flux entering D above its LCL was added to the *Se* term. Finally, a flux outgoing from D to the adjacent drainage channel occurred from 11 August 2015 to 17 August 2015 (6.0 L s^{-1}), reducing the slope of the *SP* curve just before the field drying (mid-August). After the removal of the identified *Se* fluxes from *SP*, the cumulated values of P_{bal} and P_D matched fairly well also for fields C and D (Figure 5(c) and 5(d)).

Seasonal water balance and WUE at different scales

Table 2 reports the cumulated fluxes on a seasonal basis. Values refer to the period from seeding to harvest for fields A and B (152 and 155 days, respectively), and from the very first submersion of the season (just before seeding) to harvest for fields C and D (117 days). Since the periods are different, the total amount of precipitation (*R*) and evapotranspiration (*ET*) also differs slightly among the fields.

Table 2 | Seasonal water balance terms (mm) and WUE (%) for fields A, B, C, D and for the group of paddies ACD, computed from seeding to harvest for field A and B and from the first submersion (a few days before seeding) to harvest for fields C and D

Field	R	Q_{in}	Q_{out}	Net irr.	ΔS_s	ΔS_w	ET	SP	WUE
A	273	2,716	6	2,710	10	0	630	−2,327	21
B	273	2,067	17	2,050	13	0	635	−1,660	28
C	198	899	261	638	6	0	575	−277	66
D	198	504	501	3	19	0	575	387	275
ACD	273	1,544	230	1,315	6	0	611	−972	39

The ΔS_s and ΔS_w terms are very small and they are reported in Table 2 for the sake of completeness. Contrarily, relevant amounts and strong differences among the fields appear when comparing Q_{in}, Q_{out} and WUE.

In fields A and B, water infiltrates at a high rate; thus, fields can be dried for treatment application just by stopping the irrigation inflow for 1 or 2 days. Due to these high infiltration rates, Q_{out} was always close to zero. On the contrary, the farmer used the irrigation outlets of C and D during the season to control the water level in the field and to dry the fields as required by treatments. In the case of field D, Q_{out} was practically equal to Q_{in}, due to the presence of lateral fluxes. High irrigation inputs and negligible discharges led to high net irrigations ($Q_{in} - Q_{out}$) required by A (2,710 mm) and B (2,050 mm), whereas net irrigation input was only 640 mm in C and almost no irrigation was required in D.

Considering only the irrigation management adopted in the fields, DFL applied to A and B resulted in lower WUEs (21% and 28%, respectively) compared to the traditional WFL technique adopted in C and D (66% and 275%, respectively). Although some studies comparing WFL and DFL report small water savings in the case of DFL (e.g., Borrell *et al.* 1997; Cesari de Maria *et al.* 2017), DFL showed a much lower WUE than WFL in this study, due to the topographic position of fields A and B and to the high permeability of their soils. Since farmers often select fields where applying DFL management on the basis of the permeability of their soils and the groundwater table depth (tillage operations must be conducted in these fields by means of common agricultural machinery), DFL applied in the real agricultural world may often not achieve WUEs observed in experimental tests.

Leaving aside the peculiar condition of field D, WUEs observed for fields A, B and C are in good agreement with results of other studies. With respect to experiments performed in Northern Italy, WUE, according to data from Zhao *et al.* (2015) ranged from a minimum of 26% to a maximum of 56%, similar to values computed from Karpouzas *et al.* (2005), varying between 28% and 60% in two subsequent years. On the other hand, values closer to the lower bound are reported by Cesari de Maria *et al.* (2017) and Aguilar & Borjas (2005), who observed WUEs between 17% and 27% for flooded rice paddies. As found in many other countries, a lower WUE of paddies compared to other cereals can be observed also in Northern Italy. In particular, the WUE of maize, which is the major crop cultivated in the Po river plain, usually ranges between 30% and 50% when border irrigation is applied and between 70% and 80% in the case of sprinkler irrigation (data from regional reports).

Since the very high WUE of field D is due to extra water inputs provided by the continuous flooding of fields A and C, water balance terms and WUE were computed also considering the group of paddies A, C and D as a whole (ACD in Table 2). Due to the internal reuse of seepage fluxes occurring between paddies, the net irrigation of the group of fields ACD (around 1,550 mm) was indeed lower than that measured for A and B, while WUE was found to be around 40%.

CONCLUSIONS

This study focused on the quantification of water balance terms and WUE of four rice fields, characterized by different elevations ($A \cong B + C > D$) and located in the main Italian rice basin (Lomellina region), during the agricultural season 2015. Irrigation water management was dry-seeding

and delayed flooding (DFL) in fields A and B, and water seeding and continuous flooding (WFL) in fields C and D. Since fields A, C and D lie on the same slope (while B is separated by a deep drainage channel) and their water dynamics are often interconnected, the three fields were also considered as a whole (ACD) in the study.

During the entire agricultural season, a higher net irrigation was required by the upslope fields A (2,710 mm) and B (2,050 mm) compared to downslope fields C (638 mm) and D (nearly 0 mm). The small values for fields C and D are not only due to a low soil permeability and a shallow groundwater table, but also to the occurrence of incoming seepage fluxes from upslope fields.

By measuring or estimating the different terms of the water balance for each field, the seepage and percolation flux (*SP*) was computed as the residual term of the water balance equation. Following a Darcy-based approach, percolation could be distinguished from net seepage. Throughout the flooding periods, *SP* was found to be practically coincident with the percolation term for the upslope fields (A and B), and no significant seepage fluxes were identified for these fields. On the contrary, seepage provided a large amount of water to the downslope field D, which was characterized by an irrelevant vertical percolation due to both a low soil permeability and a very shallow groundwater table, most likely maintained by the percolation of the upslope fields (A and C). Field C behaved halfway between fields A and D. The net irrigation for the group of paddies ACD reached 1,550 mm, due to the water reuse within paddies in the toposequence.

WUEs of the upslope fields (A and B) were 21–28%, field D showed a WUE >100%, while an intermediate value was found for field C (66%). Considering the irrigation management adopted in the fields, DFL applied to A and B resulted in lower WUEs compared to the traditional WFL technique adopted in C and D. This was due to the fact that, in the specific case study, topography was the dominant factor in determining the value of WUE, overwhelming all the other factors, including the irrigation management. The group ACD showed a relatively high WUE (39%), due to water reuse among fields promoted by the topographic gradient. This demonstrates that none of the fields could be considered representative of the entire paddy area, and thus, to quantify the WUE of a sequence of fields on a slope, the monitoring scale must be enlarged to include all the fields in the area.

ACKNOWLEDGEMENTS

This study was conducted in the context of the project WATPAD, funded by Fondazione Cariplo (grant no. 2014-1260) which is kindly acknowledged. We wish to thank Paolo Carnevale, owner of the Cerino farm (PV), for hosting the experimentation.

REFERENCES

Aguilar, M. & Borjas, F. 2005 Water use in three rice flooding management systems under Mediterranean climatic conditions. *Span. J. Agric. Res.* **3** (3), 344–351.

Allen, R. G., Pereira, L. S., Raes, D. & Smith, M. 1998 *Crop Evapotranspiration – Guidelines for Computing Crop Water Requirements*. FAO Irrigation and Drainage Paper 56. Food and Agriculture Organization, Rome.

Allen, R. G., Pruitt, W. O., Wright, J. L., Howell, T. A., Ventura, F., Snyder, R., Itenfisu, D., Steduto, P., Berengena, J., Yrisarry, J. B., Smith, M., Pereira, L. S., Raes, D., Perrier, A., Alves, I., Walter, I. & Elliott, R. 2006 A recommendation on standardized surface resistance for hourly calculation of reference ETO by the FAO56 Penman-Monteith method. *Agric. Water Manage.* **81**, 1–22. DOI: 10.1016/j.agwat.2005.03.007.

Borrell, A., Garside, A. & Fukai, S. 1997 Improving efficiency of water use for irrigated rice in a semi-arid tropical environment. *Field Crop Res.* **52**, 231–248.

Bouman, B. A. M., Lampayan, R. M. & Tuong, T. P. 2007 *Water Management in Irrigated Rice; Coping with Water Scarcity*. International Rice Research Institute, Los Baños.

Cabangon, R. J., Tuong, T. P., Castillo, E. G., Bao, L. X., Lu, G., Wang, G. H., Cui, L., Bouman, B. A. M., Li, Y., Chen, C. & Wang, J. 2004 Effect of irrigation method and N-fertilizer management on rice yield, water productivity and nutrient-use efficiencies in typical lowland rice conditions in China. *Paddy Water Environ.* **2**, 195–206.

Cesari de Maria, S., Rienzner, M., Facchi, A., Chiaradia, E. A., Romani, M. & Gandolfi, C. 2016 Water balance implications of switching from continuous submergence to flush irrigation in a rice-growing district. *Agric. Water Manage.* **171**, 108–119. DOI: 10.1016/j.agwat.2016.03.018.

Cesari de Maria, S., Bischetti, G. B., Chiaradia, E. A., Facchi, A., Miniotti, E. F., Rienzner, M., Romani, M., Tenni, D. & Gandolfi, C. 2017 The role of water management and environmental factors on field irrigation requirements and

water productivity of rice. *Irrig. Sci.* **35**, 11–26. DOI: 10.1007/s00271-016-0519-3.

Chiaradia, E. A., Facchi, A., Masseroni, D., Ferrari, D., Bischetti, G. B., Gharsallah, O., Cesari de Maria, S., Rienzner, M., Naldi, E., Romani, M. & Gandolfi, C. 2015 An integrated, multisensor system for the continuous monitoring of water dynamics in rice fields under different irrigation regimes. *Environ. Monit. Assess.* **187** (9), 586. DOI: 10.1007/s10661-015-4796-8.

Dong, B., Molden, D., Loeve, R., Li, Y. H., Chen, C. D. & Wang, J. Z. 2004 Farm level practices and water productivity in Zanghe Irrigation System. *Paddy Water Environ.* **2**, 217–226.

Dunn, B. W. & Gaydon, D. S. 2011 Rice growth, yield and water productivity responses to irrigation scheduling prior to the delayed application of continuous flooding in south-east Australia. *Agric. Water Manage.* **98**, 1799–1807.

FAO 1979 *Land Evaluation Criteria for Irrigation. Report of an Expert Consultation, 27 February–2 March, 1979*. World Soil Resources Report No. 50. Food and Agriculture Organization, Rome, p. 219.

FAOSTAT 2013 *Food and Agriculture Organization of the United Nations, Statistics Division*. Download data: http://faostat3.fao.org/download/Q/QC/E (accessed January 2015).

Hafeez, M. M., Bouman, B. A. M., Van de Giesen, N. & Vlek, P. 2007 Scale effects on water use and water productivity in a rice-based irrigation system (UPRIIS) in the Philippines. *Agric. Water Manage.* **92**, 81–89.

Karpouzas, D., Ferrero, A., Vidotto, F. & Capri, E. 2005 Application of the RICEWQ-VADOFT model for simulating the environmental fate of pretilachlor in rice paddies. *Environ. Toxicol. Chem.* **24** (4), 1007–1017.

Playán, E., Pérez-Coveta, O., Martínez-Cob, A., Herrero, J., García-Navarro, P., Latorre, B., Brufau, P. & Garcés, J. 2008 Overland water and salt flows in a set of rice paddies. *Agric. Water Manage.* **95**, 645–658.

Reynolds, W. D. & Elrick, D. E. 2002 Constant head soil core (tank) method. In: J. H. Dane & C. Topp (eds), *Methods of Soil Analysis, Part 4 – Physical Methods*. SSSA book series: 5. Soil Science Society of America, Madison, WI, USA, p. 804.

Rizzo, A., Boano, F., Revelli, R. & Ridolfi, L. 2013 Role of water flow in modeling methane emissions from flooded paddy soils. *Adv. Water Resour.* **52**, 261–274.

Schmitter, P., Zwart, S. J., Danvi, A. & Gbaguidi, F. 2015 Contributions of lateral flow and groundwater to the spatio-temporal variation of irrigated rice yields and water productivity in a West-African inland valley. *Agric. Water Manage.* **152**, 286–298.

Sharma, P. K., Bhushan, L., Ladha, J. K., Naresh, R. K., Gupta, R. K., Balasubramanian, B. V. & Bouman, B. A. M. 2002 Crop-water relations in rice-wheat cropping under different tillage systems and water management practices in a marginally sodic, medium-textured soil. In: B. A. M. Bouman, H. Hengsdijk, B. Hardy, P. S. Bindraban, T. P. Tuong & J. K. Ladha (eds), *Water-wise Rice Production*. International Rice Research Institute, Los Baños, pp. 223–235.

Singh, A. K., Choudhury, B. U. & Bouman, B. A. M. 2002 Effects of rice establishment methods on crop performance, water use, and mineral nitrogen. In: B. A. M. Bouman, H. Hengsdijk, B. Hardy, P. S. Bindraban, T. P. Tuong & J. K. Ladha (eds), *Water-wise Rice Production*. International Rice Research Institute, Los Baños, pp. 237–246.

Tabbal, D. F., Bouman, B. A. M., Bhuiyan, S. I., Sibayan, E. B. & Sattar, M. A. 2002 On-farm strategies for reducing water input in irrigated rice; case studies in the Philippines. *Agric. Water Manage.* **56**, 93–112.

Ten Berge, H. F. M., Jansen, D. M., Rappoldt, K. & Stol, W. 1992 *The Soil Water Balance Module SAWAH: User's Guide and Outline*. CABO-TPE Simulation Reports, Vol. 22.

Tsubo, M., Basnayake, J., Fukai, S., Sihathep, V., Siyavong, P., Sipaseuth & Chanphengsay, M. 2006 Toposequential effects on water balance and productivity in rainfed lowland rice ecosystem in Southern Laos. *Field Crop. Res.* **97**, 209–220.

Tuong, T. P. & Bhuiyan, S. I. 1999 Increasing water-use efficiency in rice production: farm levels perspectives. *Agric. Water Manage.* **40**, 117–122.

Tuong, P., Bouman, B. A. M. & Mortimer, M. 2005 More rice, less water – integrated approaches for increasing water productivity in irrigated rice-based systems in Asia. *Plant Prod. Sci.* **8**, 231–241. DOI: 10.1626/pps.8.231.

Wallace, J. S. 2000 Increasing agricultural water use efficiency to meet future food production. *Agr. Ecosyst. Environ.* **82**, 105–119.

Wopereis, M. C. S., Bouman, B. A. M., Kropff, M. J., ten Berge, H. F. M. & Maligaya, A. R. 1994 Water use efficiency of flooded rice fields I. Validation of the soil-water balance model SAWAH. *Agr. Water Management* **26** (4), 277–289.

Zhao, Y., De Maio, M., Vidotto, F. & Sacco, D. 2015 Influence of wet-dry cycles on the temporal infiltration dynamic in temperate rice paddies. *Soil Till. Res.* **154**, 14–21.

First received 13 July 2017; accepted in revised form 6 May 2018. Available online 23 May 2018